STEP BUNCHING AND SOLUTION FLOW

A. A. Chernov[*]

BAE Systems North America at Marshall Space Flight Center, NASA,
Mail Code SD46, MSFC, AL 35812, USA

Some general unresolved problems of crystal growth from solution are briefly mentioned in Secs 1 and 2. Sec 3 presents the basic physical reasons for step bunching on a growing vicinal crystal surface in presence of solution flow. In Sec 4, influence of turbulent solution flow on an average steady state bunch width is discussed. The model takes into account the fact that solution flowing over a step bunch is depleted because of higher step density within the bunch. The solution depleted by this denser step train is dragged by the flow and simultaneously expands due to turbulent diffusion into the viscous sublayer adjacent to the growing crystal surface up to the boundary between the sublayer and bulk turbulent flow. Time required for this diffusion multiplied by the solution rate at the sublayer external boundary provides an estimate for the limiting length Λ over which a step density perturbation influences solution concentration down the stream. Thus, finite thickness of the viscous sublayer determines typical bunch width Λ, $\sim v/u_\tau$ along the solution flow, where v is solution viscosity and u_τ is friction velocity of the turbulent flow. This estimate is in reasonable agreement with the experiment, but full scale solution is still a challenge.

1. Introduction – general notes on crystal growth from solutions

Crystal growth from solution attracts much closer attention during the last decades than before for both practical and fundamental scientific reasons.

Fundamental questions on growth kinetics not yet answered for solution growth are numerous. To what extent solution layer adjacent to a crystal face is ordered? What are concentrations of crystallizing ions and/or molecules and impurities on crystal interface, and what positions do these species take? Do these species move on the surface? Does surface diffusion contribute to the growth rate of steps and faces? How can we predict more precisely interfacial energies, kinetic coefficients and growth rates of kinks, steps and faces? These are just a few questions among many that may be asked on the interface of kinetics and thermodynamics.

Creation of defects in growing crystals remains an important fundamental and practical issue. What processes control creation and density of point defects (impurities, solvent species, vacancies), dislocations, twins and mosaicity? How can we get better insight into these processes and defect contribution to crystal performance?

In biomacromolecular crystals [1], the role of conformational changes within the macromolecules that may affect diffraction quality of these crystals is not known. Far insufficient insight into intermacromolecular binding and origin of crystal imperfection is being compensated by years of hard work on empirical screening through many thousands of conditions for each protein by biochemists and crystallographers. Still, mainly "low hanging fruits" are available on that level. Lack of understanding and, consequently, of a more rational approach, makes protein crystallization a major bottleneck for structural biology. The reason is that very perfect crystals are needed to reveal, by x-ray diffraction, three-dimensional structures of biomacromolecules – hundreds of thousands of different proteins, nucleic acids and their complexes, like viruses.

---

[*] Corresponding author: Alexander.Chernov@msfc.nasa.gov

Major practical incentive for inorganic crystal growth from solutions still comes from non-linear optics. Traditional demand for the high quality KDP family crystals [2] was enhanced by using these crystals to double or triple laser frequency in laser ignited nuclear fusion. For instance, at the Lawrence Livermore National Laboratory, ten powerful laser beams, ~1 m in diameter each, should go through the frequency multiplying crystals and focus on a mm-scale target. The conventional KDP growth rate of ~1 mm/day requires a year-scale time to grow the 50 cm size crystals. These crystals must be flawless and inclusion free to sustain gigawatt range laser radiation. Therefore, any unexpected failure of the growth process, which is very probable to occur during the year-scale time, would mean that the crystal is lost. As a result, fast crystal growth technology emerged [2-4] with the face growth rates up to several cm/day in the laboratory scale experiments, and ~1 cm/day in production runs. This big achievement required technology eliminating powerful step bunches, up to ~mm high, on the growing crystal surfaces fraught with inclusions trapped by these step bunches. Step bunches trap point defects in amounts different from that incorporated by single steps. This difference contributes to striations [5] sectoriality and vicinal sectoriality within the grown crystals, which induce variations in refractive index. Unlike striations induced by variations in external temperature, composition and liquid flows, the bunching related striations can not be eliminated by stabilization of external conditions and convection flows. Both inclusions and step bunches themselves come from morphological instability of a growing crystal face, i.e. from the intrinsic growth kinetics.

The term, "morphological instability" means that an arbitrary perturbation of the growing interface shape does not extinguish in time but, rather, increases its amplitude. As soon as the growing vicinal (stepped) interface lost its stability, step bunches appear and stay on the growing interface. Onset and behavior of this dissipative structure will be discussed in this paper in Secs 3 and 4. In Sec 2, some related features of solution growth are briefly discussed.

2. Basic framework of step-step interactions

Morphological instability is essentially different for molecularly rough and smooth interface. The former type is often realized at the boundary between crystal and melt in a chemically simple system characterized by low entropy of fusion and, thus, the (bond strength/thermal energy) ratio below unity [6-10]. Metals are typical examples. On the contrary, the boundary between a crystal and a chemically complex flux is usually smooth since it is characterized by the (surface energy per molecule/kT) ratio exceeding several units or more. Numerous examples are provided by close-packed crystal interfaces characterized by simple Miller idices in contact with solution. New layers, limited by steps typically containing numerous kinks – the only growth sites – should be generated on the smooth surfaces to make it grow. Either screw dislocations or two-dimensional nuclei – islands of these new layers – are the step generators. The generation process is slow as compared to the molecular attachment process so that the singular surface grows much slower than the rough (non-singular) surface of any orientation. On the rough surfaces, kink density is of the order of reciprocal molecular density on the surface. This kink density on rough surfaces is practically independent of surface orientation so that growth shape is spherical or elliptical. Morphological instability of the spheres results in conventional dendrites. Morphological instability of flat rough interface results in lamellar or cellular structures. The only stabilization factor preventing creation of dendrites, lamellar or cellular structures is surface energy. Vast literature addressing such Mullins-Sekerka instabilities is reviewed in [11].

Singular, smooth interfaces behave differently. For smooth faces, interfacial kinetics and its strong anisotropy often play a crucial role, providing much stronger stabilization than the surface energy [12]. Morphological evidences of the instabilities are also different. Step bunching, rather than lamellar or cellular structures, emerges from instability of singular crystal faces. Step propagation kinetics and step density are crucial for onset of the bunching instability.

Onset and further behavior of step bunches is determined by kinetic interaction between steps, due to overlapping between their diffusion fields. Indeed, if a group of steps, for any reason, get closer to one another, the steps within the group compete for the nutrient supply and, therefore, move slower. The rare steps behind this group still move faster to catch up and join the retarded group. In

this sense, the bunching is similar to traffic jams: the shorter the distance between cars, the slower they move [13-15]. The kinetic interaction between steps stems from the step kinetics. The latter is controlled by the rate at which a step accommodates crystallizing species and by the interstep distances, i.e. kinetic coefficient for step propagation and step density.

If the step rate, υ, and step density on a vicinal crystal face, p/h (h is the step height and p is the vicinal surface slope) are known, the face growth rate, R, follows the evident kinematic relationship:

$$R = p\upsilon. \tag{1}$$

If steps are generated by a screw dislocation, creating a vicinal hillock on the face, then p is just an average slope of this hillock, $p \cong 10^{-2}\text{-}10^{-3}$. If steps are generated by two-dimensional nucleation, the local step density (local slope p) enters eq. (1) [10]. This slope has macroscopic sense, also, if nucleation occurs preferentially in regions of high supersaturation, e.g., near crystal edge [1, 10]. The simplest kinetic coefficient, β, for the face growth is $\beta = p\beta_{st}$, where β_{st} is the step kinetic coefficient or reciprocal resistance to crystallization at the step. This kinetic coefficient determines mass balance at the growing step [15]:

$$D\partial C / \partial r = \beta_{st}(C - C_e), \tag{2}$$

where r is radial distance from the step. It is important to remind that the kinetic coefficient should relate crystallization flux to the step ($D\partial C/\partial r$ or $\omega\upsilon$) to the supersaturation $C\text{-}C_e$ right at the step, not to the supersaturation averaged over the growing surface.

Table 1. Kinetic coefficients β_{st} and vicinal slopes p.

SUBSTANCE, FACE	β_{st}, cm/s	p	$p\beta_{st}$, cm/s
ADP, KDP, DKDP (100) NH$_4$H2PO$_4$, KH$_2$PO$_4$	$(5\text{-}12) \times 10^{-2}$	$3\times10^{-4}\text{-}8 \times 10^{-3}$	10^{-4} - 10^{-3}
ADP (101)	0.4×10^{-1}	$10^{-4}\text{–} 5 \times 10^{-3}$	$4 \times 10^{-5}\text{-}5 \times 10^{-3}$
BaNO$_3$ (111)	1.3×10^{-2}	$(3\text{-}15) \times 10^{-4}$	$4 \times 10^{-6}\text{-}2 \times 10^{-5}$
KAl (SO$_4$)$_2\bullet$12H$_2$O (111) alums	8×10^{-2}	$(0.4\text{-}3.5) \times 10^{-3}$	$3 \times 10^{-5}\text{-}3 \times 10^{-4}$
Y$_3$Fe$_5$O$_{12}$ (110), (211)		$(0.3\text{-}3) \times 10^{-2}$	$(0.4\text{-}1) \times 10^{-3}$
(YSm)$_3$(FeGa)$_5$O$_{12(}$111)	1.4×10^{-2}		10^{-2}
(EuYb)$_3$Fe$_5$O$_{12}$(111)			$(0.1\text{-}3) \times 10^{-3}$
a) lysozyme (101) 14,300*	$2\text{-}20 \times 10^{-4}$	$(1.1\text{-}1.5) \times10^{-2}$	$3\text{-}30 \times 10^{-6}$
a) lysozyme (110) 14,300	$2\text{-}3 \times 10^{-4}$	$(1.0\text{-}1.5) \times10^{-2}$	$3\text{-}30 \times 10^{-6}$
b) canavalin 147,000	9×10^{-4}	9×10^{-3}	9×10^{-6}
b) thaumatin 22,000	2×10^{-4}	2D nucleation	
c) catalase 25,000	3.2×10^{-5}	2D nucleation	
d) STMV 1,600,000	$(4\text{-}8) \times 10^{-4}$	2D nucleation	
e) ferritin 480,000	6×10^{-4}	2D nucleation	

References: *Figures at proteins show molecular weight (Da)

Inorganic:
A.A. Chernov, J. Cryst. Growth, **118** (1992) 333,
P.G. Vekilov, Yu. G. Kuznetsov, A.A. Chernov, J. Cryst. Growth, **121** (1992) 643.
Proteins:
a). P.G. Vekilov, M. Ataka, T. Katsura, J. Cryst. Growth **130** (1993) 317.
b). Y.G. Kuznetsov, A.J. Malkin, A. Greenwood, A. McPherson, J. Struct. Biol., **114** (1995) 184;
c). T.A. Land, J.J. DeYoreo, J.D. Lee, Surf. Sci. 1997, **84**, 136-155.
d). A.J. Malkin, et al., *Phys. Rev. Lett.* **75** (1995) 2781
e). S.-T. Yau, B.R. Thomas and P.G. Vekilov, *Phys. Rev. Lett.* **85** (2000) 356

Experimental data on β_{st}, p and growth modes are summarized in Table 1. Much lower figures for β_{st} for proteins may be ascribed to entropy constraints associated with large molecular size and asymmetric shape of the biomacromolecules. Also, the area per intermolecular contact in proteins may reach several percent of macromolecular surface, 10^3Å^2 or more and, thus, is also associated with high potential dehydration barrier, like with inorganic salts in aqueous solutions. Biomacromolecules are typically stable in a narrow range of temperature (~0-40 ℃) and there are no direct reliable measurements of the activation energy.

In many cases, growth kinetics corresponds to the simplest way of direct incorporation of crystallizing species from solution to the kink sites at steps [2,15]. This model is also supported by the fact that micromorphology of a growing face does depend on solution flow [16,17]. Alternatively, adsorption on interstep terraces and surface diffusion is considered even in solution growth [18,19]. For instance, the average step rate, υ, depends on the average vicinal slope, p, on the (101) face of ADP ($NH_4 KH_2 PO_4$) stronger that it may be expected from the model of direct incorporation by steps on a regular step train. Within the framework of local kinetic coefficient, this dependence was approximated by [19].

$$\upsilon\,(p) = \upsilon_o/(1+Kp) \qquad\qquad (3)$$

Here, υ_o is velocity of an isolated step. The constant is estimated [20] to be $K \sim 10^2\text{-}10^3$ so that at typical $p = 10^{-2}\text{-}10^{-3}$ the product $Kp \sim 1$. For an infinite equidistant train of elementary steps of height h, the average vincinal slope, $\bar{p}$, and kinetic coefficient β_{st} in an infinite stagnant solution occupying semispace above the interface, Kp in eq. (3) should be replaced by $(\beta_{st}\,h/D)\,\ln\left|\bar{p}\right|^{-1}$ and is practically independent on the vicinal slope, $\bar{p}$ [12]. Also, with $\beta_{st} = 0.1$ cm/s, $h = 10^{-7}$ cm, $\bar{p} \cong 10^{-2}\text{-}10^{-3}$ and bulk diffusivity $D = 10^{-5}$ cm^2/s one has $(\beta_{st}h/D)\ln\left|\bar{p}\right|^{-1} \cong 5\times10^{-3}$. However, the $\upsilon(p)$ dependence might be different if train of elementary steps is replaced by train of step bunches (Sec. 3). Nevertheless, a possibility of combined surface and bulk diffusion [18, 19] remains an option.

The dependence, eq. (3), is in agreement with dependence of the average propagation rate, υ, of a step bunch on the local slope, p, $(p > \bar{p})$ within the bunch. This dependence was measured by high precision interferometry for step bunches propagating over the steep vicinal hillock slope on the (101) face of KDP (KH_2PO_4) crystal in flowing solution [19, 21, 22]. Therefore, besides the scientific and practical interest mentioned in the beginning, behavior of step bunches may shed a light on the long standing problem of the bulk vs. surface diffusion.

In solution growth, the step bunching is much less understood than that in vapor growth and related epitaxies [23-29] since bulk diffusion and incorporation at steps are more important. Roles of surface diffusion and existence of Schwoebel asymmetry [30] are still not clear. Nevertheless, bunching in solution was addressed since long ago [31-35].

Earlier studies assumed that step bunch (and real macrosteps) might be considered as an entity of a height essentially exceeding lattice parameter (i.e. elementary step height) and, thus, propagating at velocity inversely proportional to its height – because of overlapping of bulk or surface diffusion fields of elementary steps and their mutual retardation [15]. Then, since bunch heights are not equal to one another, the propagation speeds are different so that the bunches must coalesce. If splitting of bunches is ignored, the average height increases $\sim x^{1/2}$, where x is the path covered by the sequence of bunches [15]. Step-step interaction via their bulk and surface diffusion field in application to biomacromolecular crystals was modeled [36] revealing enhanced instability only with respect to finite amplitude perturbations. Stability of an elementary step with respect to its meandering within the growth plane in flowing solution was analyzed analytically [37].

Bunching was observed to be enhanced by impurities. One of the suggested mechanisms is that impurity stoppers hindering step propagation are adsorbed on interstep terraces: the wider the terrace, the longer it is exposed to impurity adsorption, the larger the stopper density, the stronger the impurity stoppers diminish bunch propagation rate, the higher are the bunches [38,39]. In this model, the average bunch/macrostep height should also infinitely increase $\sim\ln x$, as compared to $x^{1/2}$ mentioned earlier.

3. Onset of bunching

As it was mentioned above, importance of bulk diffusion for step bunching follows directly from dependence of bunching behavior on solution flow. This dependence was found originally on the (100) face of ADP ($NH_4 H_2 PO_4$) crystal growing from solution flowing parallel to the face as shown in Fig. 1 by bold white arrows [16]. The Fig. 1 shows one vicinal conical hillock occupying the whole (100) face, ~6 × 6 mm^2 in size. The hillock is generated by dislocation step source in the center and is shown by the black arrow.
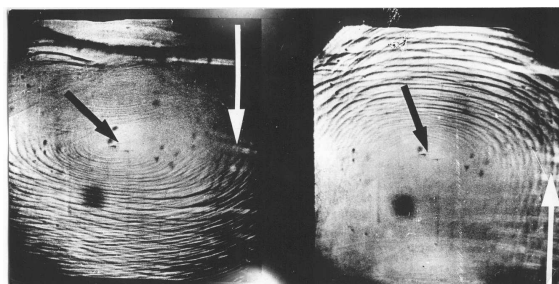
Fig. 1. Flow dependent step bunching on the (001) face of $NH_4H_2PO_4$ (ADP) crystal. One dislocation hillock, with apex shown by black arrow, occupies the whole face ~5 mm wide. White arrow shows solution flow velocity. Ripples are step bunches. The bunches are developed on the downstream slope of the hillock. When direction of solution flow changes to the opposite, bunches disappear on the now upstream slope and appear on the now downstream slope after ~1 minute.

The hillock slope where steps are moving in the same direction as the solution flows is rippled, i.e. step bunches are formed. The opposite slope of the same hillock, where the steps and solution flow in opposite directions, does not show visible bunching. When direction of solution flow is switched to the opposite, ripples disappear on the now up-stream slope and develop on the now down-stream slope. This flow-induced morphology change is completely reversible [16]. Onset of morphological instability phenomenon was understood in terms of solution flow within diffusion boundary layer [17,40-43]. To highlight this mechanism, vicinity of the corrugated crystal – solution interface is shown in Fig. 2 in cross-section normal to the surface and steps on this surface. Weak corrugation may be induced by variations in step source activity, in solution supersaturation, by presence of local step stoppers on the surface, or just by random meandering of elementary steps. Inhomogeneous step distribution on the corrugated surface induces inhomogeneous distribution of concentration over this surface: the concentration is lower where density of elementary steps absorbing the crystallizing species is higher, i.e. over the bunches, B, in Fig. 2. Similarly, over the flatter, low step density segments, F, concentration is higher as shown by various shadow intensity in Fig. 2. If solution flows to the right, as shown in Fig. 2 by the arrow u, the enriched solution from the F regions of lower step density first comes, and is discharging at the surface profile protrusions, i.e. at the rear of each bunch, B. This local increase in superstauration increases propagation rate of steps forming these protrusions and, therefore, the protrusion slopes. Similarly, the solution depleted over the bunch B comes first to the depressions and aggravates these depressions. Thus, if the solution flows down the step flow it, indeed, should cause instability. Analogously, if the step and solution flow directions are anti-parallel, the interface is stabilized.

If solution is completely stagnant while the growth or dissolution step flow still exists, the situation is similar to the flow of ideal liquid in the direction opposite to the step flow. Thus, the step motion itself may stabilize the growing or dissolving interface in stagnant solutions – self stabilization may occur [43]. At conventional supersaturations of 1-5%, the step rates are of the order of $10^{-5} \div 10^{-4}$ cm/s. Therefore, even the slow solution flows of this order of magnitude may affect the self-stabilization effect.
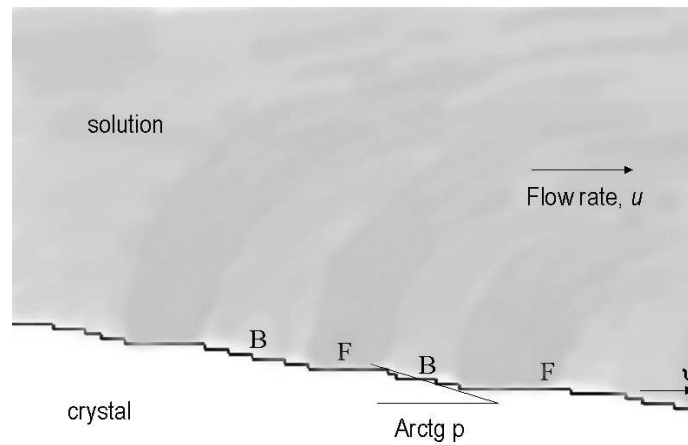
Fig. 2. Schematic of solute concentration distribution over stepped vicinal face with varying step density. Solute concentration is symbolized by background intensity. In the immediate interface vicinity, the concentration is maximal where step density is minimal, and vice versa.

Non-linear, S-shaped, dependence of face growth rate on supersaturation, typical if impurities are present in the system, enhance instability. Namely, step bunches on the (100) ADP face appear preferentially within the supersaturaion range near $\sigma = (C - C_e)/C_e \cong 1.5 \times 10^{-2}$, where the normal growth rate steeply increases. This bunching occurs independently of the solution flow direction and velocity [44]. At other supersaturations, the flow still influences onset of bunching [41, 44].

The impurity effect on bunching at least partly follows from superlinear $R(\sigma)$ dependence originating from steep superlinear increase of the step rate in the supersaturation range where the step breaks through the fence of stoppers or do not allow enough time for the impurity species to be adsorbed on terraces and steps [42]. Indeed, a periodic perturbation of a flat vicinal, i.e. equidistant step train, leads to (periodic) local slope variation and thus to the corresponding perturbation in the concentration field above this growing surface. Within the strong superlinear $R(\sigma)$ dependence, the amplitude of the perturbed concentration wave is larger than that at weaker $R(\sigma)$ dependence. Correspondingly, onset of instability should be enhanced, though specific impurity related instability mechanism should be involved. In this case, the impurity induced bunching found in experiment is not as sensitive to the solution flow as it is in the theory – it is observed at any flow direction [44]. This discrepancy is still a challenge.

Another type of step bunching on the (100) KDP face, probably also related to impurities, happens preferentially within two azumuthal sectors of a large elliptical growth hillock, the sectors being centered at the hillock apex. The bunches filling these two sectors are oriented along the direction of maximal growth rate, i.e. propagate in the direction of the minimal rate (ref. [2], Fig. 2.45).

Recently developed phase-shift interferometry allows to reveal bunch formation to the accuracy of ~ 5 nm in bunch height [21]. Growth hillock interferogram of the (101) face of KDP is viewed in Fig. 3a [21]. It consists of three slopes of which the upper left is the most shallow while the lower is the steepest out of the three. Enlarged images from different portions of the vicinal slopes are presented in Fig. 3 b-d. The lineage structures in c, d are step bunches. Recording surface height z normal to the face allows to quantitatively characterize surface profile, $z(x)$, along the coordinate x normal to the mutually parallel bunches within the growth plane. The profile and its Fourier spectrum are presented in Fig. 4. First measurements show that typical wavelength of ripples (reciprocal wavenumber) decreases as the flow rate increases and eq. (3) holds with p being local slope within the bunches [45]. It was also found that on vicinal hillocks on the (101) KDP face, usually not very sensitive to impurities, the flow induced bunching is reversed: bunches appear when the directions of

the step propagation and solution flow are anti-parallel. This happens, however, only at low supersaturations and also might be associated with traces of impurities.
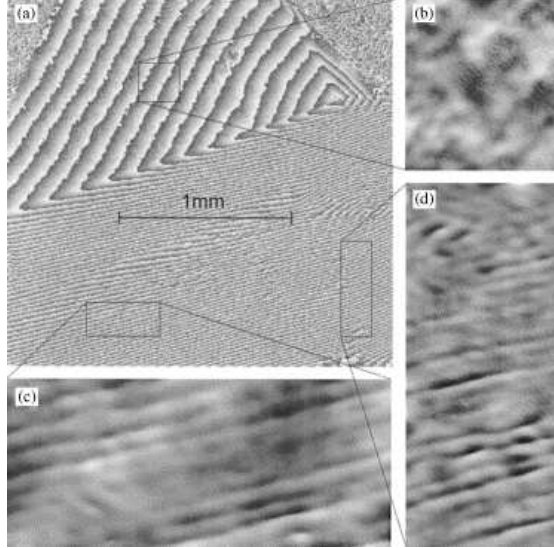

Fig. 3. High precision phase shift interferometry of a dislocation growth hillock on the (101) KH$_2$PO$_4$ (KDP) face (a). The hillock has three different slopes: average step density is proportional to the interference fringe density. Solution flows down to the fringe flow on the steepest hillock. Zooming in for different areas are shown in b, c and d. Step bunches are seen on c and d as darker bands, but not on b.

The $\upsilon(p)$ dependence, eq. (3), has not yet been theoretically understood. It may come from both bulk and surface diffusion. In case of bulk diffusion, an analogy between elementary and macrostep trains may be expected. This analogy assumes that the bunch width, Λ, is shorter than the interbunch distance, that local bunch slope, p, is proportional to the average slope, $\overline{p}$, and that the stagnant boundary layer is thicker than the interbunch distance. Then, the elementary step height, h, should be replaced by the bunch height, Λp, so that $Kp \cong (\beta_{st}\Lambda p / D)\ln p^{-1}$. Alternatively, in this expression, $\beta_{st}p$ may be considered as kinetic coefficient of the bunch. Within these assumptions, $K = (\beta_{st}\Lambda / D)\ln p^{-1}$. At $\Lambda = 20 - 200$ μm, $\beta_{st} = 0.1$ cm/s, $\overline{p} \cong 7 \cdot 10^{-3}$, D = 10^{-5} cm^2/s, one obtains $K = (\beta_{st}\Lambda / D)\ln p^{-1} \cong 10^2$ - 10^3. This estimate is encouraging for bulk diffusion model, though the whole problem still waits for consistent analysis. The diffusion field around step bunches, taking into account not stagnant, but laminar or turbulent boundary layer, should be carefully analyzed, since interaction between elementary steps and step bunches may be expected to be stronger in the flowing, as compared to the stagnant solution. This expectation comes from the stabilization and destabilization effect of solution flow [2,16]. Qualitatively, the effect of solution flow on step-step interaction resembles the effect of the wind on the air pollution level in a city: if the wind is blowing from a poorly managed chemical factory miles away, the city is strongly polluted. However, in the absence of the wind, or with the wind blowing in the opposite direction, the pollution may be barely detectable.

4. Developed instability and turbulence [45]

As step bunches develop, they do not create any regular sequence. Rather, lower steps typically moving faster split and run away from the larger bunches, join the preceeding bunches,

etc.(we do not consider here the step retardation by impurities [1] [46]). Similar behavior was observed during vapor growth [15], molecular beam and liquid phase [5] epitaxy. In other words, the bunching dissipative structure is dynamic. Properties of these structures in solutions are poorly understood. Numerous studies of bunch behavior in vapor phase epitaxy [23-30] do not help much because step-step interaction may be different in solution since transport in the bulk solution is heavily involved. This transport influence seems to be noticeably different in laminar and turbulent solution flow.
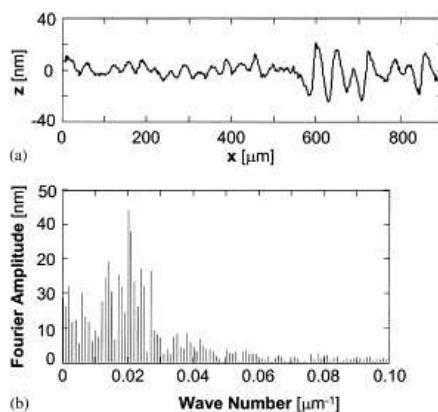
Fig. 4. Profile of the bunched slope (a) and Fourier spectrum of this profile (b).

Recent studies [45] include observation of developed bunches of the type shown in Fig. 4 [21]. In particular, it was found that the average bunch height does not increase when the bunch covers a distance of ~1.5 mm. This distance is, of course, short as compared to the cm or even tens of cm range typically covered by step bunches over the growing faces of large crystals. However, high resolution of $\pm$ 5nm in step height achieved in phase shift interferometry [21, 22] provides a hope that it captures the real trend in the self similar scaling of the bunch height behavior. This trend, occurring at the solution flow rate up to 1 m/s, suggests that step and bunch coalescence is compensated by bunch decay. One of the other important findings is that increase of flow rate from ~60 to ~120 cm/s decreases the average bunch width from about 200 to 50 μm. This width decrease is accompanied by decrease in the average bunch height of about twice.

Theoretical description of the developed dissipative bunch structures and its dependence on solution flow does not yet exist. However, we may put forward the following hypothesis addressing physics of the phenomena. We believe that the bunch width should be of the order of the length Λ at which the bunch front (area F., Fig. 5a) grows at supersaturation essentially influenced by the major, steeper portion RF of the bunch. This influence is brought about by the solution flowing down the step stream and depleted with respect to the nutrient consumed by steps within RF where the step density is higher. As soon as the step bunch is formed as a result of instability, the front steps should propagate at lower supersaturation, being fed by depleted solution "wind" blowing from the steep bunch. Thus, these front steps should move slower, making the bunch even steeper. However, the average step density over distances much longer than the typical bunch width, Λ, should remain constant over the whole macroscopic face. This average step density is generated by the step source, producing this macroscopic vicinal face. To keep the average step density constant, the step density in the bunch front should decrease – when step retardation caused by depleted "wind" becomes insufficient to compete with the supply of crystallizing species from the bulk solution through the boundary layer. Then, the front steps run away from the steeper bunch. In other words, the bunch width is limited by the characteristic length,Λ, past a point (R in Fig. 5a) where the step density changes from one lower value to the higher. Weakening of the "wind" depletion may also facilitate

---

[1] In presence of impurities, elementary steps may propagate at lower rates than step bunches, or do not move at all, as it was observed on the (100) KDP face in presence of Fe^{3+}. This effect probably comes from inability of the elementary step to "bury" the adsorbed layer of impurities. On the other hand, the gain in free energy for the step bunch is proportional to its height, so that the bunch is able to propagate burying the adsorbed impurities.

the bunch splitting. To estimate Λ, we assume that the new, higher step density is kept constant at any larger distance $x > 0$. The concentration balance between depletion by the higher step density and supply from the solution bulk occurs by diffusion and convection transport within the viscous boundary layer separating bulk turbulent flow from the solid wall, i.e. from the growing crystal surface.
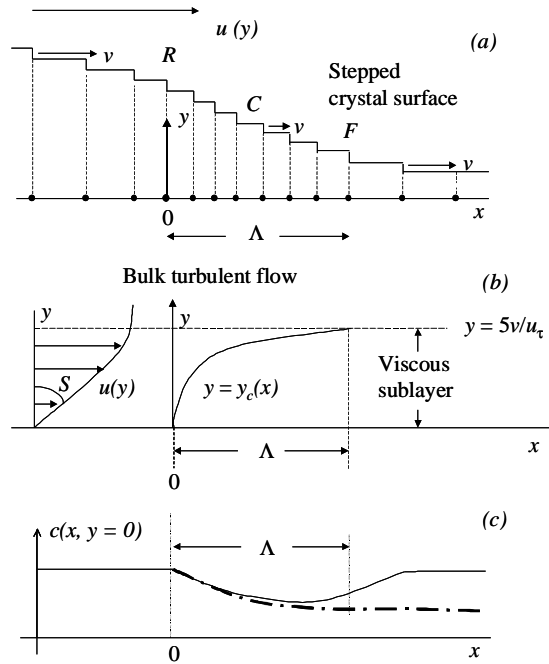

Fig. 5. Step bunch and related concentration distribution. a. Step bunch on a gorwing vicinal face: upper drawing – stepped profile; lower drawing – projections of steps on the singular crystal face as solid points on the x-axis. b. Viscous sublayer adjacent to the growing stepped vicinal interface. On the left – linear velocity distribution $u(y)$ within the layer with the beginning on logarithmic dependence in the bulk turbulent flow. Schematic trajectory $y_c(x)$ separates, in the flowing solution, the area with two different concentrations. Concentration on the left from the trajectory is determined by the average step density at $x < 0$. Concentration on the right from any $y = y_c(x)$ is depleted because at $x = 0$, solution meets the crystal surface with higher step density. The concentration change at this trajectory is steep close to the interface and continuously smears out as the distance y from the crystal surface increases. Similar trajectory may be drawn from any point x on the surface where step density changes. c. Concentration at the growing surface. The lower dash-dotted line schematically represents concentration resulted from matching two semi-infinite vicinal faces with lower step density on the left and higher on the right from $x = 0$. The full line corresponds to the step bunch.

In the turbulent flow, the viscous sublayer adjacent to the crystal surface is known to extend over the distance y from the wall (see ref [47]):

$$0 < y < y_b \cong 5v/u_\tau \tag{4}$$

Here, v is molecular viscosity of solution and u_τ is the friction velocity. This velocity is defined via the energy density, ρu_τ^2, dissipated in the boundary layer transferring the shear stress from the bulk turbulent flow in a pipe of sufficiently large radius R_o to the wall of this pipe. The friction velocity is related to the average flow velocity, $\bar{u}$, through the pipe [48]:

$$u_\tau = 0.18 \, (v/R_o)^{1/8} \, \bar{u}^{7/8}. \tag{5}$$

Within the viscous sublayer, eq. (4), there exist noticeable velocity fluctuations in the y direction normal to the wall. Small liquid volumes moving randomly to and from the solid wall carry different concentrations and, thus, induce solution mixing. This turbulent mass transfer stems from the same fluctuations in the y-component of the flow velocity near the wall that transfers flow momentum tangential to the wall and results in the stress that flowing liquid acts on the wall with. Therefore, the turbulent diffusivity, D_t, similar to the turbulent viscosity and heat diffusivity may be written as

$$D_t = \kappa_D u_\tau y, \tag{6}$$

For the turbulent viscosity, $v_t = 0.41\ u_\tau y$ and thermal diffusivity, $a_t = 0.47\ u_\tau y$ (ref. [47], eq. (18. 38)). For further estimates, we take the numerical coefficient in eq. (6) to be $\kappa_D = 0.5$. Like turbulent viscosity, mass diffusivity is the linear function of distance y to the wall. Thus, at the distance $y \gg y_o = D_o/\kappa_D u_\tau$, molecular diffusivity, $D_o \cong 10^{-5}$ cm^2/s, is insignificant as compared to the turbulent mixing mass transfer within the viscous boundary sublayer. At $\bar{u} \cong 100$ cm/s, $v = 10^{-2}$ cm^2/s, $R_o \cong 1$ cm, eq. (5) provides $u_\tau = 5.8$ cm/s, so that viscous sublayer, eq. (4), expands up to $y_b \cong 90$ mkm. At $D_o \cong 10^{-5}$ cm^2/s, the molecular diffusivity is important only at the distances $y < y_o \cong 0.03$ mkm from the surface, while in the rest of the viscous sublayer, the turbulent mixing transport prevails. Though molecular diffusion is dominant only within very thin layer y_o, the diffusion resistance of this layer is naturally not as dramatically different as the difference between y_o and y_b - because molecular diffusivity is much lower than the turbulent one. Total diffusion resistance of the boundary layer may be found by solving the diffusion equation with the total diffusivity $D = D_o + \kappa_D u_\tau y$. The so found characteristic diffusion rate through the whole boundary layer (its kinetic coefficient) is

$$\kappa_D u_\tau / \ln\ [1 + 5\kappa_D v/D_o] \cong 0.37\ \text{cm/s}, \tag{7}$$

while the molecular diffusion rate kinetic coefficient is $D_o/y_o \cong 3.3$ cm/s. In other words, resistance for the molecular diffusion, $y_o/D_o \cong 0.3$ s/cm is about 10% of the whole resistance given by the reciprocal of expression (7). It is worthy to underline that the kinetic coefficient for the boundary layer, eq. (7), strongly exceeds the interface kinetic coefficient, $\beta_{st}\bar{p} \cong 3 \cdot 10^{-4} cm/s$. Therefore, the overall growth rate is totally controlled by interface kinetics, so that the instability phenomena discussed here are realized due to relative supersaturation variations over different parts of the growing interface. In other words, though absolute superasaturation at the interface is practically equal to that in the solution bulk, these are the relative variations that make a difference.

Let us now estimate the average bunch width, Λ, Fig. 5. Fig. 5a shows the step bunch profile, assuming all steps are normal to the drawing plane. The x-axis positive direction coincides with both the step and solution flows. Each step is projected on the x-axis as a point. Since the average vicinal slope is $p < 10^{-2}$ and the bunch height typically does not exceed 100 nm $\cong 0.1\ \mu$m, we can consider the growing interface as a flat wall with inhomogeneously distributed linear links – elementary steps. Fig. 5b presents the solution viscous sublayer, $5v/u_\tau$ thick, eq. 4, within which the flow velocity, $u(y)$, increases linearly with the distance from the crystal surface (left hand side of the figure). The flow rate within the bulk turbulent flow increases much slower with y (as $\ln y$) so that large-scale fluctuations mix the solution in the bulk flow much more intensively. Therefore, concentration at $y \geq 5v/u_\tau$ may be taken as a constant equal to the prepared concentration of the mother liquor.

Solution arriving at the bunch rear, R (Fig. 5a), is characterized by a concentration $c(y)$, $y < 5v/u_\tau$, corresponding to the average concentration accounting for the presence of numerous other bunches up the stream. Meeting the higher step density at R, solution concentration at the surface decreases by some δc, a difference that is proportional to the difference in the step density before and after R. This rather sharp change of concentration is dragged by the flowing solution, simultaneously diffuses away from the interface and continuously smears out. The trajectory of the center of the border between the intact solution coming from the left from R and depleted solution on the right is shown in Fig. 5b by the curve $y = y_c(x)$. Depleted solution at a point x, diffusing from the surface, covers the distance $y_c = 2\sqrt{Dt}$, where D is the solute diffusivity and t is the time that is needed for

solution to reach point x at the height y_c. Evidently, $t \cong x/u(y) = x/Sy$, where the shear flow $S \equiv \partial u/\partial y = u_\tau^2 /v$ [47]. Therefore, the border trajectory $y_c(x)$ may be approximated by equation

$$y_c = 2\sqrt{(D_o + \kappa_D u_\tau y_c)x/ Sy_c}. \qquad (8)$$

The trajectory $y_c(x)$ reaches the external border of the viscous sublayer $y = 5v/u_\tau$ at a distance $x = \Lambda$ such that

$$5v/u_\tau \cong 2\sqrt{\kappa_D u_\tau \Lambda / S} \qquad (9)$$

where we assume $y >> y_o$, so that molecular diffusivity is ignored. From eq. (9),

$$\Lambda = (25/4\kappa_D)v/u_\tau \qquad (10)$$

i.e. Λ is proportional to the thickness of the viscous sublayer. Since $u_\tau \sim \bar{u}^{7/8}$, following eq. (5), Λ is about reciprocal to solution velocity. At $\kappa_D = 0.5$, $v = 10^{-2}$ cm^2/s, $\bar{u} = 120$ cm/s, $u_\tau = 5.8$ cm/s, one has $\Lambda \cong 190$ µm. At $\bar{u} = 60$ cm/s, $u_\tau = 3.6$ cm/s, one has $\Lambda \cong 340$ µm. Experimental figures are about four times larger, but also show decrease of the typical bunch width with increasing flow rate. A more systematic theory should be developed to adjust numerical coefficient in eq. (10).

Eq (10) estimates the length of the transient region within which concentration reaches a new steady state level corresponding to the new step density abruptly changed at $x = 0$ (region R in Fig. 5a), and is kept artificially constant all the way down the stream. The concentration profile for that model is shown by the dash-dotted line in Fig. 5c. In reality, however, the depletion induced by the step density increase at $x > 0$, decreases the step velocities at $x > 0$ and, therefore, causes further rise in the step density, etc. On the other hand, the requirement of constant average vicinal slope, i.e. the average step density, should limit this step density rise, ending up with the step bunch of a final width as shown by Fig. 5a. Therefore, the actual bunches should be narrower than that predicted by eq. (10). The corresponding concentration profile should follow the solid curve in Fig. 5c. Again, more rigorous analysis coupling the step density with the diffusion field in the boundary layer is required.

The approach explored above essentially uses two features of turbulent flow – a finite and rather small thickness of viscous boundary sublayer and turbulent diffusivity, which exceeds molecular diffusivity by two or three orders of magnitude, and increases with the distance from the wall. In laminar flow, diffusion in boundary should also enhance interaction between steps, but there is no the cut-off effect at $y = y_b$ we have used here to estimate Λ. Not less important, another difference is that molecular diffusibility relevant for laminar flow is about a thousand times lower than the turbulent diffusivity and does not depend on the distance to the growing surface.

5. Conclusions

Step bunching is a ubiquitous phenomenon of morphological instability on growing vicinal crystal faces resulting in striations and trapping of inclusions by growing crystals. Solution flowing in the same direction as the steps, propagate results in step bunching on a vicinal face. If the solution and step flows are antiparallel, the vicinal face remains stable.

Under conditions of developed bunching instability, the typical bunch width and height decrease when the solution velocity increases. The effect seems to be essentially connected with the turbulent character of the flow. Typical bunch width should be limited by the thickness of viscous sublayer $\sim v/u_\tau$ and, as such, decreases when solution flow increases.

References

[1] P. G. Vekilov, A. A. Chernov, Sol. St. Phys. **57**, 1-147 (2002).

[2] L. N. Rashkovich, KDP-Family Single Crystals. Bristol: Adam Hilger (1991).

[3] V. I. Bespalov, V. I. Bredikhin, V. I. Katsman, V. P. Ershov, L. A. Lavrov, J. Cryst. Growth **82**, 776 (1987).

[4] J. J. DeYoreo, Z. V. Reck, N. P. Zaitseva, B. W. Woods, J. Cryst. Growth **166**, 291 (1995).

[5] E. Bauser, Atomic Mechanisms in Semiconductor Liquid Phase Epitaxy, in Handbook of Crystal Growth, D. T. J. Hurle, Editor, North Holland: Amsterdam p. 879-911 (1994).

[6] W. K. Burton, Cabrera, N. &. Frank, F.C., Phil. Trans. Roy. Soc. London Ser. A. **243**, 299- 360 (1951).

[7] J. Frenkel, Phys. J. USSR **1**, 498-510 (1932).

[8] K. A. Jackson, Interface structure, in Growth and Perfection of Crystals, R. H. Doremus, B. W. Roberts, and D. Turnbull, Editors, Chapman and Hill: London. p. 319-323 (1958).

[9] S. T. Chui, J. D. Weeks, Phys. Rev. B **14**, 4978 (1978).

[10] A. A. Chernov, Modern Crystallography III, Crystal Growth, Berlin: Springer (1984).

[11] S. R. Coriell, G. B. McFadden, in Handbook of Crystal Growth, D. T. J. Hurle, Editor, North Holland: Amsterdam (1993).

[12] A. A. Chernov, J. Crystal Growth. **24/25**, 11-31 (1974).

[13] F. C. Frank, On the kinmatic theory of crystal growth and dissolution processes, in Growth and Perfection of Crystals, R. H. Doremus, B. W. Roberts, and D. Turnbull, Editors, Wiley: New York. p. 411-417 (1958).

[14] N. Cabrera, D. A. Vermileya, The growth of crystals form solution, in Growth and Perfection of Crystals, R. H. Doremus, B. W. Roberts, and D. Turnbull, Editors, Wiley: New York (1958).

[15] A. A. Chernov, Sov. Phys. Uspekhi. **4**, 116-148 (1961).

[16] A. A. Chernov, Y. G. Kuznetsov, I. L. Smol'sky, V. N. Rozhanskii, Sov. Phys Crystallogr. **31**, 705-711 (1986).

[17] A. A. Chernov, J. Crystal Growth. **118**, 333-347 (1992).

[18] G. H. Gilmer, R. Ghez, N. Cabrera, J. Crystal Growth **8**, 79-93 (1971).

[19] P. G. Vekilov, Y. G. Kuznetsov, A. A. Chernov, J. Crystal Growth **121**, 643-655 (1992).

[20] P. G. Vekilov, B. R. Thomas, F. Rosenberger, J. Phys. Chem. **102**, 5208-5216 (1998).

[21] N. A. Booth, A. A. Chernov, P. G. Vekilov, J. Crystal Growth **237-239**, 1818-1824 (2002).

[22] N. A. Booth, B. Stanojev, A. A. Chernov, P. G. Vekilov, Rev. Sci. Instr. **73**, 3540-3545 (2002).

[23] M. Sato, M. Uwaha, Y. Saito, Phys. Rev. B **62**, 8452-8472 (2000).

[24] M. Uwaha, Y. Saito, M. Sato, J. Cryst. Growth **146**, 164-172 (1995).

[25] F. Liu, H. Metiu, Phys. Rev. E **49**, 2601 (1994).

[26] K. Fujita, M. Ichikawa, S. Stoyanov, Phys. Rev. B **60**, 16006-16012 (1999).

[27] S. Stoyanov, Surf. Sci. **464**, L715-L718 (2000).

[28] A. Videcoq, A. Pimpinelli, M. Vladimirova, Appl. Phys. Sci. **177**, 213-220 (2001).

[29] P. Tijecor, P. Smilauer, C. J. Roberts, B. A. Joyce, Phys. Rev. B **59**, 2341-2345 (1999).

[30] R. L. Schwoebel, E. J. Shipsey, J. Appl. Phys. **37**, 3682-3686 (1966).

[31] D. G. Vlachos, L. D. Schmidt, R. Aris, Phys. Rev. B **47**, 4896-4909 (1993).

[32] I. Sunagawa, Morphology of minerals, in Morphology of Crystals Part B, I. Sunagawa, Editor, Terra Sci. Pub.; D. Riedel Pub Co: Dordrecht. p. 509-587 (1987).

[33] I. Sunagawa, Morphology of crystal faces, in Morphology of Crystals Part A, I. Sunagawa, Editor, Terra Sci. Pub.; D. Riedel Pub Co: Dordrecht. p. 321-365 (1987).

[34] D. Elwell, H.J. Scheel, Crystal Growth from High Temperature Solutions. London: Academic Press. (1975).

[35] A. A. Chernov, T. Nishinaga, Growth shapes and their stability at anisotropic interface kinetics: theoretical aspects for solution growth, in Morphology of Crystals, I. Sunagawa, Editor, TERRA Sci. Publ. Co.: Tokyo. p. 207-267 (1987).

[36] F. Rosenberger, H. Lin, P. G. Vekilov, Phys. Rev. E **59**, 3155-3164 (1999).

[37] S. Y. Potapenko, J. Cryst. Growth **158**, 346-358 (1996).

[38] J. P. Van der Eerden, H. Mueller-Krumbhaar, Physical Review Letters **57**, 2431-2433 (1986).

[39] J. P. Van der Eerden, H. Mueller-Krumbhaar, Electrochemica Acta **31**, 1007 (1986).

[40] B. T. Murray, S. R. Coriell, A. A. Chernov, G. B. McFadden, Journal of Crystal Growth **218**, 434-446 (2000).

[41] S. R. Coriell, B. T. Murrary, A. A. Chernov, G. B. McFadden, J. Crystal Growth **169**, 773-785 (1996).

[42] S. R. Coriell, A. A. Chernov, B. T. Murray, G. B. McFadden, J. Crystal Growth **183**, 669-682 (1998).

[43] A. A. Chernov, S. R. Coriell, B. T. Murray, J. Cryst. Growth **132**, 405-412 (1993).

[44] L. N. Rashkovich, B. Y. Shekunov, J. Crystal Growth **100**, 133-144 (1990).

[45] N. A. Booth, A. A. Chernov, P. G. Vekilov. (In preparation).

[46] T. A. Land, T. L. Martin, S. Potapenko, G. T. Palmore, J. J. De Yoreo, Nature **399**, 442 - 445 (1999).

[47] H. Schlichting, K. Gersten, Boundary Layer Theory, 8th edition, ed. Springer. Berlin (2000).

[48] H. Schlichting, Boundary Layer Theory, 7th Edition, ed. Springer. Berlin (1979).